Optics and Photonics Journal, 2014, 4, 246-269
Published Online September 2014 in SciRes. http://www.scirp.org/journal/opj
http://dx.doi.org/10.4236/opj.2014.49025

Calculation of Atomic Data and Gain Coefficient for XUV & Soft X-Ray Laser Emission from Ge XXIII

Wessameldin S. Abdelaziz

National Institute of Laser Enhanced Sciences, Cairo University, Giza, Egypt
Email: wessamlaser@yahoo.com

Received 21 June 2014; revised 18 July 2014; accepted 12 August 2014

Abstract

Energy levels, transition probabilities, oscillator strengths, and collision strengths have been calculated for transitions in Ne-like Ge. The data refer to a 241 fine-structure levels belonging to the configurations $1s^2\,2s^2\,2p^5nl$, $1s^2\,2s^1\,2p^6nl$ (n = 3, 4, 5, 6; l = s, p, d, f, g and h), which have been calculated by the fully relativistic flexible atomic code (FAC). These data are used in the determination of the reduced population for the 241 fine structure levels and gain coefficients over a wide range of electron densities (from $2 \times 10^{+20}$ to $4 \times 10^{+22}$ cm^{-3}) and at various electron plasma temperatures (650, 850, 1050, 1250, 1450, 1650, 1850) eV by using the MATLAB R2013a Computer program for solving simultaneous coupled rate equations. The reduced population for the 241 fine structure levels the gain coefficients for those transitions with positive population inversion factor are determined and plotted against the electron density.

Keywords

Energy Levels, Transition Probabilities, Oscillator Strengths, Collision Strengths

1. Introduction

The concept for x-ray lasers went back to the 1965s, when it was based on the laser-produced plasmas by electron de-excitation having a promising interest science, which was first proposed by the Soviet scientists Gudzenko and Shelepin [1]. They thought that the short wavelength laser in the x-ray region of the electromagnetic spectrum needed a large energy gap which was sustained in the highly ionized ions. After ionization, in the equilibrium plasma, ions having specific number of electrons such as 2 (helium-like), 10 (neon-like), 28 (nickel-like) and 46 (palladium-like) were relatively stable and survived in a wide range of temperature and density [2] [3]. X-ray

How to cite this paper: Abdelaziz, W.S. (2014) Calculation of Atomic Data and Gain Coefficient for XUV & Soft X-Ray Laser Emission from Ge XXIII. *Optics and Photonics Journal*, **4**, 246-269. http://dx.doi.org/10.4236/opj.2014.49025

lasers pumping methods are electron collisional excitation, photo excitation, charge transfer, electron collisional recombination and de-electronic recombination pumping using a picosecond chirped pulse amplification (CPA) pulse [4], a capillary discharge [5] [6] and a free electron laser. However, the electron collisional excitation pumping of the inner shell and outer shell of highly ionization states have shown a more stable and a higher output [7] [8]. Thus, the electron collisional pumping proved to be the most efficient method in producing the x-ray lasers.

Experimentally there exist in the literature some studies trying to develop high-efficiency X-ray laser with significant gain, for example, [3] [9] proposed the original mechanism for demonstrating X-ray lasing by resonant photo pumping. Several authors during the past three decades [10] [11] have studied this lasing mechanism experimentally and theoretically, in the hope of developing high-efficiency X-ray laser. In another study by Qi, N. and Krishnan, M. [12], the shortest wavelength at which the significant gain had been measured using the resonant photo pumping was in the beryllium-like carbon at 2163 Å, which was far from the X-ray spectral region.

In this paper, we calculate energy levels for 241 fine-structure states using a fully relativistic approach based on Dirac equation (see **Table 1**). Weighted Oscillator strengths, spontaneous radiative decay rates are calculated in the single multipole approximation (see **Table 2**), and Collision strengths by electron impact using the factorization-interpolation method are calculated in the distorted wave approximation. Effective collision strengths are calculated by interpolating the data from the collision strengths and integrating over Max wellian distribution at different temperatures. Rate coefficients are calculated from effective collision strengths using a formula that will be described later in this paper. Then, we predict the reduced population and gain coefficient for Ge XXIII by a steady state equation in the collisional radiative model after achieving a population inversion between the allowed transition states.

Table 1. Energy levels of Ge XXIII, and their threshold energies (in eV).

Index	State Configuration	J^{π}	FAC	COWAN	NIST	Exp.	CIV3	MCDF	RCI
1	$2p^6$	0^e	0.00000E+00	0.00000E+00	0.00000E+00	0.00000E+00	0.00000E+00	0.00000E+00	0.00000E+00
2	$2p_{3\backslash 2}3s_{1\backslash 2}$	2^o	1.23421E+03	1.23585E+03		1.236122E+03	1.23596E+03	1.234804E+03	1.236931E+03
3	$2p_{3\backslash 2}3s_{1\backslash 2}$	1^o	1.23709E+03	1.23863E+03	1.23900E+03	1.238602E+03	1.23859E+03	1.237659E+03	1.239498E+03
4	$2p_{1\backslash 2}3s_{1\backslash 2}$	0^o	1.26664E+03	1.26835E+03		1.268358E+03	1.26828E+03	1.267259E+03	1.269494E+03
5	$2p_{1\backslash 2}3s_{1\backslash 2}$	1^o	1.26822E+03	1.26994E+03	1.27009E+03	1.269598E+03	1.26978E+03	1.268864E+03	1.270625E+03
6	$2p_{3\backslash 2}3p_{1\backslash 2}$	1^e	1.27690E+03	1.27848E+03	---	1.278277E+03	1.27857E+03	1.277620E+03	1.280475E+03
7	$2p_{3\backslash 2}3p_{1\backslash 2}$	2^e	1.28046E+03	1.28213E+03	---	1.281997E+03	1.28213E+03	1.280943E+03	1.283104E+03
8	$2p_{3\backslash 2}3p_{3\backslash 2}$	3^e	1.28642E+03	1.28801E+03	---	1.288196E+03	1.28801E+03	1.286986E+03	1.288182E+03
9	$2p_{3\backslash 2}3p_{3\backslash 2}$	1^e	1.28726E+03	1.28859E+03	---	1.288196E+03	1.28869E+03	1.287800E+03	1.288267E+03
10	$2p_{3\backslash 2}3p_{3\backslash 2}$	2^e	1.29059E+03	1.29201E+03	1.29204E+03	1.291915E+03	1.29190E+03	1.291035E+03	1.291087E+03
11	$2p_{3\backslash 2}3p_{3\backslash 2}$	0^e	1.30216E+03	1.30328E+03	---	1.303074E+03	1.30354E+03	1.302522E+03	1.301413E+03
12	$2p_{1\backslash 2}3p_{1\backslash 2}$	1^e	1.31186E+03	1.31352E+03	---	1.314232E+03	1.31355E+03	1.312405E+03	1.314407E+03
13	$2p_{1\backslash 2}3p_{3\backslash 2}$	1^e	1.31985E+03	1.32137E+03	---	1.321671E+03	1.32122E+03	1.320429E+03	1.322501E+03
14	$2p_{1\backslash 2}3p_{3\backslash 2}$	2^e	1.32083E+03	1.32231E+03	1.32254E+03	1.322911E+03	1.32229E+03	1.321340E+03	1.323593E+03
15	$2p_{1\backslash 2}3p_{1\backslash 2}$	0^e	1.33447E+03	1.33333E+03	1.33333E+03	1.332830E+03	1.33321E+03	1.332304E+03	1.334537E+03
16	$2p_{3\backslash 2}3d_{3\backslash 2}$	0^o	1.34070E+03	1.34234E+03	---	1.342749E+03	1.34218E+03	1.341534E+03	1.343407E+03
17	$2p_{3\backslash 2}3d_{3\backslash 2}$	1^o	1.34247E+03	1.34422E+03	1.34473E+03	1.343989E+03	1.34403E+03	1.343296E+03	1.345574E+03
18	$2p_{3\backslash 2}3d_{5\backslash 2}$	4^o	1.34553E+03	1.34748E+03	---	---	1.34724E+03	1.346399E+03	1.348306E+03
19	$2p_{3\backslash 2}3d_{5\backslash 2}$	2^o	1.34575E+03	1.34753E+03	---	1.347708E+03	1.34730E+03	1.346560E+03	1.348784E+03
20	$2p_{3\backslash 2}3d_{3\backslash 2}$	3^o	1.34594E+03	1.34772E+03	---	1.347708E+03	1.34779E+03	1.346843E+03	1.348794E+03
21	$2p_{3\backslash 2}3d_{3\backslash 2}$	2^o	1.34871E+03	1.35031E+03	---	1.350188E+03	1.35025E+03	1.349561E+03	1.351217E+03

Continued

22	$2p_{3/2}3d_{5/2}$	3^o	1.35077E+03	1.35267E+03	---	1.352668E+03	1.35230E+03	1.351588E+03	1.353658E+03
23	$2p_{3/2}3d_{5/2}$	1^o	1.35938E+03	1.35991E+03	1.36085E+03	1.361346E+03	1.36075E+03	1.360284E+03	1.362151E+03
24	$2p_{1/2}3d_{3/2}$	2^o	1.37811E+03	1.37920E+03	---	---	1.37955E+03	1.378922E+03	1.380718E+03
25	$2p_{1/2}3d_{5/2}$	2^o	1.37971E+03	1.38104E+03	---	---	1.38101E+03	1.380575E+03	1.382465E+03
26	$2p_{1/2}3d_{5/2}$	3^o	1.38086E+03	1.38195E+03	---	1.383664E+03	1.38231E+03	1.381764E+03	1.383652E+03
27	$2p_{1/2}3d_{3/2}$	1^o	1.38931E+03	1.38884E+03	1.38825E+03	1.391103E+03	1.39058E+03	1.389940E+03	1.392453E+03
28	$2s_{1/2}3s_{1/2}$	1^e	1.42808E+03	---	---	---	1.40081E+03	---	1.430234E+03
29	$2s_{1/2}3s_{1/2}$	0^e	1.43744E+03	---	---	---	1.40856E+03	---	1.438962E+03
30	$2s_{1/2}3p_{1/2}$	0^o	1.47300E+03	---	---	---	1.43866E+03	---	1.474996E+03
31	$2s_{1/2}3p_{1/2}$	1^o	1.47381E+03	---	1.47132E+03	---	1.43962E+03	---	1.476085E+03
32	$2s_{1/2}3p_{3/2}$	2^o	1.48066E+03	---	---	---	1.44646E+03	---	1.482977E+03
33	$2s_{1/2}3p_{3/2}$	1^o	1.48318E+03	---	1.48074E+03	---	1.44867E+03	---	1.485577E+03
34	$2s_{1/2}3d_{3/2}$	1^e	1.53678E+03	---	---	---	1.49950E+03	---	1.539105E+03
35	$2s_{1/2}3d_{3/2}$	2^e	1.53722E+03	---	---	---	1.50003E+03	---	1.539522E+03
36	$2s_{1/2}3d_{5/2}$	3^e	1.53813E+03	---	---	---	1.50093E+03	---	1.540470E+03
37	$2s_{1/2}3d_{5/2}$	2^e	1.54524E+03	---	---	---	1.50787E+03	---	1.547695E+03
38	$2p_{3/2}4s_{1/2}$	2^o	1.67001E+03	1.67259E+03	---	---	---	---	---
39	$2p_{3/2}4s_{1/2}$	1^o	1.67092E+03	1.67259E+03	1.67250E+03	---	---	---	---
40	$2p_{3/2}4p_{1/2}$	1^e	1.68781E+03	1.69062E+03	---	---	---	---	---
41	$2p_{3/2}4p_{1/2}$	2^e	1.68868E+03	1.69125E+03	---	---	---	---	---
42	$2p_{3/2}4p_{3/2}$	3^e	1.69117E+03	1.69380E+03	---	---	---	---	---
43	$2p_{3/2}4p_{3/2}$	1^e	1.69150E+03	1.69405E+03	---	---	---	---	---
44	$2p_{3/2}4p_{3/2}$	2^e	1.69258E+03	1.69497E+03	---	---	---	---	---
45	$2p_{3/2}4p_{3/2}$	0^e	1.69841E+03	1.69999E+03	---	---	---	---	---
46	$2p_{1/2}4s_{1/2}$	0^o	1.70254E+03	1.70497E+03	---	---	---	---	---
47	$2p_{1/2}4s_{1/2}$	1^o	1.70295E+03	1.70497E+03	1.70466E+03	---	---	---	---
48	$2p_{3/2}4d_{3/2}$	0^o	1.71168E+03	1.71460E+03	---	---	---	---	---
49	$2p_{3/2}4d_{3/2}$	1^o	1.71237E+03	1.71521E+03	---	---	---	---	---
50	$2p_{3/2}4d_{5/2}$	4^o	1.71336E+03	1.71608E+03	---	---	---	---	---
51	$2p_{3/2}4d_{3/2}$	3^o	1.71340E+03	1.71621E+03	---	---	---	---	---
52	$2p_{3/2}4d_{5/2}$	2^o	1.71356E+03	1.71631E+03	---	---	---	---	---
53	$2p_{3/2}4d_{3/2}$	2^o	1.71440E+03	1.71704E+03	---	---	---	---	---
54	$2p_{3/2}4d_{5/2}$	3^o	1.71516E+03	1.71772E+03	---	---	---	---	---
55	$2p_{3/2}4d_{5/2}$	1^o	1.71893E+03	1.72055E+03	1.72078E+05	---	---	---	---
56	$2p_{1/2}4p_{1/2}$	1^e	1.72080E+03	1.72379E+03	---	---	---	---	---
57	$2p_{1/2}4p_{3/2}$	1^e	1.72399E+03	1.72689E+03	---	---	---	---	---
58	$2p_{1/2}4p_{3/2}$	2^e	1.72433E+03	1.72708E+03	---	---	---	---	---
59	$2p_{3/2}4f_{5/2}$	1^e	1.72480E+03	1.72713E+03	---	---	---	---	---
60	$2p_{3/2}4f_{5/2}$	4^e	1.72501E+03	1.72742E+03	---	---	---	---	---
61	$2p_{3/2}4f_{7/2}$	2^e	1.72515E+03	1.72746E+03	---	---	---	---	---

Continued

62	$2p_{3/2}4f_{7/2}$	5^e	1.72516E+03	1.72764E+03	---	---	---	---	---
63	$2p_{3/2}4f_{7/2}$	3^e	1.72574E+03	1.72798E+03	---	---	---	---	---
64	$2p_{3/2}4f_{5/2}$	2^e	1.72585E+03	1.72807E+03	---	---	---	---	---
65	$2p_{3/2}4f_{5/2}$	3^e	1.72591E+03	1.72810E+03	---	---	---	---	---
66	$2p_{3/2}4f_{7/2}$	4^e	1.72613E+03	1.72817E+03	---	---	---	---	---
67	$2p_{1/2}4p_{1/2}$	0^e	1.72618E+03	1.72838E+03	---	---	---	---	---
68	$2p_{1/2}4d_{3/2}$	2^o	1.74573E+03	1.74855E+03	---	---	---	---	---
69	$2p_{1/2}4d_{5/2}$	2^o	1.74642E+03	1.74941E+03	---	---	---	---	---
70	$2p_{1/2}4d_{5/2}$	3^o	1.74687E+03	1.74986E+03	---	---	---	---	---
71	$2p_{1/2}4d_{3/2}$	1^o	1.74908E+03	1.75109E+03	1.75090E+03	---	---	---	---
72	$2p_{1/2}4f_{5/2}$	3^e	1.75784E+03	1.76052E+03	---	---	---	---	---
73	$2p_{1/2}4f_{7/2}$	4^e	1.75816E+03	1.76073E+03	---	---	---	---	---
74	$2p_{1/2}4f_{5/2}$	2^e	1.75818E+03	1.76084E+03	---	---	---	---	---
75	$2p_{1/2}4f_{7/2}$	3^e	1.75824E+03	1.76085E+03	---	---	---	---	---
76	$2p_{3/2}5s_{1/2}$	2^o	1.86014E+03	---	---	---	---	---	---
77	$2p_{3/2}5s_{1/2}$	1^o	1.86061E+03	---	---	---	---	---	---
78	$2s_{1/2}4s_{1/2}$	1^e	1.86083E+03	---	---	---	---	---	---
79	$2s_{1/2}4s_{1/2}$	0^e	1.86447E+03	---	---	---	---	---	---
80	$2p_{3/2}5p_{1/2}$	2^e	1.86954E+03	---	---	---	---	---	---
81	$2p_{3/2}5p_{1/2}$	1^e	1.86965E+03	---	---	---	---	---	---
82	$2p_{3/2}5p_{3/2}$	3^e	1.87079E+03	---	---	---	---	---	---
83	$2p_{3/2}5p_{3/2}$	1^e	1.87117E+03	---	---	---	---	---	---
84	$2p_{3/2}5p_{3/2}$	2^e	1.87148E+03	---	---	---	---	---	---
85	$2p_{3/2}5p_{3/2}$	0^e	1.87450E+03	---	---	---	---	---	---
86	$2s_{1/2}4p_{1/2}$	0^o	1.87921E+03	---	---	---	---	---	---
87	$2s_{1/2}4p_{1/2}$	1^o	1.87983E+03	---	---	---	---	---	---
88	$2p_{3/2}5d_{3/2}$	0^o	1.88142E+03	---	---	---	---	---	---
89	$2p_{3/2}5d_{3/2}$	1^o	1.88158E+03	---	1.88679E+03	---	---	---	---
90	$2p_{3/2}5d_{5/2}$	2^o	1.88163E+03	---	---	---	---	---	---
91	$2p_{3/2}5d_{3/2}$	3^o	1.88172E+03	---	---	---	---	---	---
92	$2p_{3/2}5d_{5/2}$	4^o	1.88173E+03	---	---	---	---	---	---
93	$2p_{3/2}5d_{3/2}$	2^o	1.88217E+03	---	---	---	---	---	---
94	$2p_{3/2}5d_{5/2}$	3^o	1.88255E+03	---	---	---	---	---	---
95	$2s_{1/2}4p_{3/2}$	2^o	1.88335E+03	---	---	---	---	---	---
96	$2s_{1/2}4p_{3/2}$	1^o	1.88338E+03	---	1.88679E+03	---	---	---	---
97	$2p_{3/2}5d_{5/2}$	1^o	1.88476E+03	---	---	---	---	---	---
98	$2p_{3/2}5f_{5/2}$	1^e	1.88719E+03	---	---	---	---	---	---
99	$2p_{3/2}5f_{5/2}$	2^e	1.88742E+03	---	---	---	---	---	---
100	$2p_{3/2}5f_{5/2}$	4^e	1.88754E+03	---	---	---	---	---	---
101	$2p_{3/2}5f_{7/2}$	5^e	1.88760E+03	---	---	---	---	---	---

Continued

102	$2p_{3\backslash2}5f_{7\backslash2}$	3^e	1.88780E+03	---	---	---	---	---	---
103	$2p_{3\backslash2}5g_{7\backslash2}$	2^o	1.88786E+03	---	---	---	---	---	---
104	$2p_{3\backslash2}5g_{9\backslash2}$	3^o	1.88795E+03	---	---	---	---	---	---
105	$2p_{3\backslash2}5f_{5\backslash2}$	3^e	1.88795E+03	---	---	---	---	---	---
106	$2p_{3\backslash2}5f_{7\backslash2}$	2^e	1.88797E+03	---	---	---	---	---	---
107	$2p_{3\backslash2}5f_{7\backslash2}$	4^e	1.88808E+03	---	---	---	---	---	---
108	$2p_{3\backslash2}5g_{7\backslash2}$	5^o	1.88817E+03	---	---	---	---	---	---
109	$2p_{3\backslash2}5g_{7\backslash2}$	3^o	1.88824E+03	---	---	---	---	---	---
110	$2p_{3\backslash2}5g_{9\backslash2}$	6^o	1.88825E+03	---	---	---	---	---	---
111	$2p_{3\backslash2}5g_{9\backslash2}$	4^o	1.88830E+03	---	---	---	---	---	---
112	$2p_{3\backslash2}5g_{7\backslash2}$	4^o	1.88842E+03	---	---	---	---	---	---
113	$2p_{3\backslash2}5g_{9\backslash2}$	5^o	1.88849E+03	---	---	---	---	---	---
114	$2p_{1\backslash2}5s_{1\backslash2}$	0^o	1.89308E+03	---	---	---	---	---	---
115	$2p_{1\backslash2}5s_{1\backslash2}$	1^o	1.89329E+03	---	---	---	---	---	---
116	$2p_{1\backslash2}5p_{1\backslash2}$	1^e	1.90155E+03	---	---	---	---	---	---
117	$2p_{1\backslash2}5p_{3\backslash2}$	2^e	1.90316E+03	---	---	---	---	---	---
118	$2p_{1\backslash2}5p_{3\backslash2}$	1^e	1.90352E+03	---	---	---	---	---	---
119	$2p_{1\backslash2}5p_{1\backslash2}$	0^e	1.90422E+03	---	---	---	---	---	---
120	$2s_{1\backslash2}4d_{5\backslash2}$	3^e	1.90492E+03	---	---	---	---	---	---
121	$2s_{1\backslash2}4d_{3\backslash2}$	1^e	1.90493E+03	---	---	---	---	---	---
122	$2s_{1\backslash2}4d_{3\backslash2}$	2^e	1.90495E+03	---	---	---	---	---	---
123	$2s_{1\backslash2}4d_{3\backslash2}$	2^e	1.90740E+03	---	---	---	---	---	---
124	$2p_{1\backslash2}5d_{3\backslash2}$	2^o	1.91418E+03	---	---	---	---	---	---
125	$2p_{1\backslash2}5d_{5\backslash2}$	2^o	1.91454E+03	---	---	---	---	---	---
126	$2p_{1\backslash2}5d_{5\backslash2}$	3^o	1.91471E+03	---	---	---	---	---	---
127	$2s_{1\backslash2}4f_{5\backslash2}$	3^o	1.91553E+03	---	---	---	---	---	---
128	$2s_{1\backslash2}4f_{7\backslash2}$	4^o	1.91561E+03	---	---	---	---	---	---
129	$2p_{1\backslash2}5d_{3\backslash2}$	1^o	1.91567E+03	---	1.91779E+03	---	---	---	---
130	$2s_{1\backslash2}4f_{5\backslash2}$	2^o	1.91624E+03	---	---	---	---	---	---
131	$2s_{1\backslash2}4f_{7\backslash2}$	3^o	1.91667E+03	---	---	---	---	---	---
132	$2p_{1\backslash2}5f_{5\backslash2}$	3^e	1.92023E+03	---	---	---	---	---	---
133	$2p_{1\backslash2}5f_{7\backslash2}$	4^e	1.92040E+03	---	---	---	---	---	---
134	$2p_{1\backslash2}5f_{5\backslash2}$	2^e	1.92046E+03	---	---	---	---	---	---
135	$2p_{1\backslash2}5f_{7\backslash2}$	3^e	1.92049E+03	---	---	---	---	---	---
136	$2p_{1\backslash2}5g_{7\backslash2}$	4^o	1.92087E+03	---	---	---	---	---	---
137	$2p_{1\backslash2}5g_{9\backslash2}$	5^o	1.92095E+03	---	---	---	---	---	---
138	$2p_{1\backslash2}5g_{7\backslash2}$	3^o	1.92159E+03	---	---	---	---	---	---
139	$2p_{1\backslash2}5g_{9\backslash2}$	4^o	1.92168E+03	---	---	---	---	---	---
140	$2p_{3\backslash2}6s_{1\backslash2}$	2^o	1.96032E+03	---	---	---	---	---	---
141	$2p_{3\backslash2}6s_{1\backslash2}$	1^o	1.96055E+03	---	---	---	---	---	---

Continued

142	$2p_{3/2}6p_{1/2}$	1^e	1.96543E+03	---	---	---	---	---	---
143	$2p_{3/2}6p_{1/2}$	2^e	1.96562E+03	---	---	---	---	---	---
144	$2p_{3/2}6p_{3/2}$	3^e	1.96636E+03	---	---	---	---	---	---
145	$2p_{3/2}6p_{3/2}$	1^e	1.96644E+03	---	---	---	---	---	---
146	$2p_{3/2}6p_{3/2}$	2^e	1.96670E+03	---	---	---	---	---	---
147	$2p_{3/2}6p_{3/2}$	0^e	1.96836E+03	---	---	---	---	---	---
148	$2p_{3/2}6d_{3/2}$	0^o	1.97209E+03	---	---	---	---	---	---
149	$2p_{3/2}6d_{3/2}$	1^o	1.97229E+03	---	---	---	---	---	---
150	$2p_{3/2}6d_{3/2}$	3^o	1.97253E+03	---	---	---	---	---	---
151	$2p_{3/2}6d_{5/2}$	4^o	1.97257E+03	---	---	---	---	---	---
152	$2p_{3/2}6d_{3/2}$	2^o	1.97259E+03	---	---	---	---	---	---
153	$2p_{3/2}6d_{5/2}$	2^o	1.97279E+03	---	---	---	---	---	---
154	$2p_{3/2}6d_{5/2}$	3^o	1.97299E+03	---	---	---	---	---	---
155	$2p_{3/2}6d_{5/2}$	1^o	1.97404E+03	---	1.97680E+03	---	---	---	---
156	$2p_{3/2}6f_{5/2}$	1^e	1.97568E+03	---	---	---	---	---	---
157	$2p_{3/2}6f_{5/2}$	4^e	1.97579E+03	---	---	---	---	---	---
158	$2p_{3/2}6f_{5/2}$	2^e	1.97580E+03	---	---	---	---	---	---
159	$2p_{3/2}6f_{7/2}$	5^e	1.97583E+03	---	---	---	---	---	---
160	$2p_{3/2}6f_{5/2}$	3^e	1.97597E+03	---	---	---	---	---	---
161	$2p_{3/2}6f_{7/2}$	3^e	1.97602E+03	---	---	---	---	---	---
162	$2p_{3/2}6p_{7/2}$	2^e	1.97605E+03	---	---	---	---	---	---
163	$2p_{3/2}6f_{7/2}$	4^e	1.97609E+03	---	---	---	---	---	---
164	$2p_{3/2}6g_{7/2}$	2^o	1.97626E+03	---	---	---	---	---	---
165	$2p_{3/2}6g_{7/2}$	5^o	1.97626E+03	---	---	---	---	---	---
166	$2p_{3/2}6h_{9/2}$	3^e	1.97627E+03	---	---	---	---	---	---
167	$2p_{3/2}6h_{11/2}$	4^e	1.97630E+03	---	---	---	---	---	---
168	$2p_{3/2}6h_{9/2}$	6^e	1.97630E+03	---	---	---	---	---	---
169	$2p_{3/2}6g_{9/2}$	6^o	1.97631E+03	---	---	---	---	---	---
170	$2p_{3/2}6g_{9/2}$	3^o	1.97631E+03	---	---	---	---	---	---
171	$2p_{3/2}6h_{11/2}$	7^e	1.97633E+03	---	---	---	---	---	---
172	$2p_{3/2}6h_{9/2}$	4^e	1.97635E+03	---	---	---	---	---	---
173	$2p_{3/2}6h_{9/2}$	5^e	1.97637E+03	---	---	---	---	---	---
174	$2p_{3/2}6g_{7/2}$	3^o	1.97638E+03	---	---	---	---	---	---
175	$2p_{3/2}6h_{11/2}$	5^e	1.97638E+03	---	---	---	---	---	---
176	$2p_{3/2}6g_{7/2}$	4^o	1.97639E+03	---	---	---	---	---	---
177	$2p_{3/2}6g_{7/2}$	6^e	1.97641E+03	---	---	---	---	---	---
178	$2p_{3/2}6g_{9/2}$	4^o	1.97642E+03	---	---	---	---	---	---
179	$2p_{3/2}6g_{9/2}$	5^o	1.97644E+03	---	---	---	---	---	---
180	$2p_{1/2}6s_{1/2}$	0^o	1.99290E+03	---	---	---	---	---	---
181	$2p_{1/2}6s_{1/2}$	1^o	1.99302E+03	---	---	---	---	---	---

Continued

182	$2p_{1/2}6p_{1/2}$	1^e	1.99809E+03	---	---	---	---	---	---
183	$2p_{1/2}6p_{3/2}$	1^e	1.99900E+03	---	---	---	---	---	---
184	$2p_{1/2}6p_{3/2}$	2^e	1.99910E+03	---	---	---	---	---	---
185	$2p_{1/2}6p_{1/2}$	0^e	1.99929E+03	---	---	---	---	---	---
186	$2p_{1/2}6d_{3/2}$	2^o	2.00505E+03	---	---	---	---	---	---
187	$2p_{1/2}6d_{5/2}$	2^o	2.00526E+03	---	---	---	---	---	---
188	$2p_{1/2}6d_{5/2}$	3^o	2.00538E+03	---	---	---	---	---	---
189	$2p_{1/2}6d_{3/2}$	1^o	2.00585E+03	---	2.00879E+03	---	---	---	---
190	$2p_{1/2}6f_{5/2}$	3^e	2.00844E+03	---	---	---	---	---	---
191	$2p_{1/2}6f_{7/2}$	3^e	2.00854E+03	---	---	---	---	---	---
192	$2p_{1/2}6f_{7/2}$	4^e	2.00854E+03	---	---	---	---	---	---
193	$2p_{1/2}6f_{5/2}$	2^e	2.00855E+03	---	---	---	---	---	---
194	$2p_{1/2}6g_{7/2}$	4^o	2.00891E+03	---	---	---	---	---	---
195	$2p_{1/2}6h_{9/2}$	4^e	2.00892E+03	---	---	---	---	---	---
196	$2p_{1/2}6s_{g7/2}$	3^o	2.00893E+03	---	---	---	---	---	---
197	$2p_{1/2}6h_{9/2}$	5^e	2.00894E+03	---	---	---	---	---	---
198	$2p_{1/2}6h_{11/2}$	5^e	2.00896E+03	---	---	---	---	---	---
199	$2p_{1/2}6g_{9/2}$	5^o	2.00896E+03	---	---	---	---	---	---
200	$2p_{1/2}6h_{11/2}$	6^e	2.00897E+03	---	---	---	---	---	---
201	$2p_{1/2}6g_{9/2}$	4^o	2.00897E+03	---	---	---	---	---	---
202	$2s_{1/2}5s_{1/2}$	1^e	2.05136E+03	---	---	---	---	---	---
203	$2s_{1/2}5s_{1/2}$	0^e	2.05274E+03	---	---	---	---	---	---
204	$2s_{1/2}5p_{1/2}$	0^o	2.06056E+03	---	---	---	---	---	---
205	$2s_{1/2}5p_{1/2}$	1^o	2.06068E+03	---	---	---	---	---	---
206	$2s_{1/2}5p_{3/2}$	2^o	2.06209E+03	---	---	---	---	---	---
207	$2s_{1/2}5p_{3/2}$	1^o	2.06247E+03	---	---	---	---	---	---
208	$2s_{1/2}5d_{3/2}$	1^e	2.07254E+03	---	---	---	---	---	---
209	$2s_{1/2}5d_{3/2}$	2^e	2.07264E+03	---	---	---	---	---	---
210	$2s_{1/2}5d_{5/2}$	3^e	2.07286E+03	---	---	---	---	---	---
211	$2s_{1/2}5d_{5/2}$	2^e	2.07389E+03	---	---	---	---	---	---
212	$2s_{1/2}5f_{5/2}$	2^o	2.07841E+03	---	---	---	---	---	---
213	$2s_{1/2}5f_{5/2}$	3^o	2.07844E+03	---	---	---	---	---	---
214	$2s_{1/2}5f_{7/2}$	4^o	2.07853E+03	---	---	---	---	---	---
215	$2s_{1/2}5f_{7/2}$	3^o	2.07871E+03	---	---	---	---	---	---
216	$2s_{1/2}5g_{7/2}$	4^e	2.07901E+03	---	---	---	---	---	---
217	$2s_{1/2}5g_{7/2}$	3^e	2.07901E+03	---	---	---	---	---	---
218	$2s_{1/2}5g_{9/2}$	5^e	2.07909E+03	---	---	---	---	---	---
219	$2s_{1/2}5g_{9/2}$	4^e	2.07909E+03	---	---	---	---	---	---
220	$2s_{1/2}6s_{1/2}$	1^e	2.15120E+03	---	---	---	---	---	---
221	$2s_{1/2}6s_{1/2}$	0^e	2.15196E+03	---	---	---	---	---	---

Continued

222	$2s_{1/2}6p_{1/2}$	0^o	2.15644E+03	---	---	---	---	---	---
223	$2s_{1/2}6p_{1/2}$	1^o	2.15652E+03	---	---	---	---	---	---
224	$2s_{1/2}6p_{3/2}$	2^o	2.15735E+03	---	---	---	---	---	---
225	$2s_{1/2}6p_{3/2}$	1^o	2.15755E+03	---	---	---	---	---	---
226	$2s_{1/2}6d_{3/2}$	1^e	2.16329E+03	---	---	---	---	---	---
227	$2s_{1/2}6d_{3/2}$	2^e	2.16336E+03	---	---	---	---	---	---
228	$2s_{1/2}6d_{5/2}$	3^e	2.16349E+03	---	---	---	---	---	---
229	$2s_{1/2}6d_{5/2}$	2^e	2.16403E+03	---	---	---	---	---	---
230	$2s_{1/2}6f_{5/2}$	2^o	2.16658E+03	---	---	---	---	---	---
231	$2s_{1/2}6f_{5/2}$	3^o	2.16660E+03	---	---	---	---	---	---
232	$2s_{1/2}6f_{7/2}$	4^o	2.16665E+03	---	---	---	---	---	---
233	$2s_{1/2}6f_{7/2}$	3^o	2.16676E+03	---	---	---	---	---	---
234	$2s_{1/2}6g_{7/2}$	3^e	2.16703E+03	---	---	---	---	---	---
235	$2s_{1/2}6g_{7/2}$	4^e	2.16703E+03	---	---	---	---	---	---
236	$2s_{1/2}6h_{9/2}$	5^o	2.16705E+03	---	---	---	---	---	---
237	$2s_{1/2}6h_{9/2}$	4^o	2.16705E+03	---	---	---	---	---	---
238	$2s_{1/2}6g_{9/2}$	5^e	2.16708E+03	---	---	---	---	---	---
239	$2s_{1/2}6h_{11/2}$	6^o	2.16708E+03	---	---	---	---	---	---
240	$2s_{1/2}6h_{11/2}$	5^o	2.16708E+03	---	---	---	---	---	---
241	$2s_{1/2}6g_{9/2}$	4^e	2.16708E+03	---	---	---	---	---	---

Index: Level index. **State Configuration**: The configuration to which the level belongs (jj-coupling). **J^π**: J is the Total angular momentum, π is the Parity. **FAC**: Energies from the FAC code (our calculation). **COWAN**: Energies from the COWAN code (also calculated). **NIST**: National Institute of Standards and Technology, http://www.nist.gov [24]. **Exp.**: Energies calculated experimentally [23]. **CIV3**: Energies from the CIV3 code [22]. **MCDF**: Energies from the MCDF code [23]. **RCI**: Energies from the RCI code [23].

Table 2. Comparison between some weighted oscillator strengths, and transition probabilities for E1 transitions of Ge XXIII.

j	i	gf (FAC)	gf (COWAN)	gf (CIV3)	gf (RCI)	A_{ji} (s^{-1}) (FAC)	A_{ji} (s^{-1}) (COWAN)	A_{ji} (s^{-1}) (CIV3)
3	1	1.29E−01	1.0139E−01	1.280E−01	----	2.86E+12	2.2503E+12	2.84E+12
5	1	8.88E−02	7.0307E−02	8.480E−02	----	2.07E+12	1.6400E+12	1.1868E+12
6	2	2.26E−01	2.5061E−01	2.257E−01	0.2685	5.96E+09	6.5800E+09	5.9267E+09
7	2	2.13E−01	2.1330E−01	2.113E−01	0.2246	3.96E+09	3.9660E+09	3.9080E+09
7	3	2.15E−01	2.2961E−01	2.185E−01	0.2204	3.51E+09	3.7720E+09	3.5940E+09
8	2	7.00E−01	7.2277E−01	7.002E−01	0.7275	1.18E+10	1.2177E+10	1.1760E+10
9	2	4.53E−04	1.1885E−04	4.000E−04	0.0001	1.85E+07	4.7833E+06	1.5900E+07
9	3	2.84E−01	2.9512E−01	2.827E−01	0.2914	1.03E+10	1.0657E+10	1.0260E+10
10	2	2.91E−01	2.9107E−01	2.923E−01	0.3092	8.02E+09	7.9700E+09	7.9360E+09
10	3	2.52E−01	2.4604E−01	2.480E−01	0.2431	6.27E+09	6.0900E+09	6.1160E+09
10	5	6.21E−04	8.1658E−04	5.000E−04	----	2.70E+06	3.4520E+06	2.3540E+06
11	3	1.08E−01	1.0495E−01	1.102E−01	0.0930	1.98E+10	1.9050E+10	2.0180E+10
11	5	1.26E−02	1.1588E−02	1.130E−02	----	6.31E+08	5.5900E+08	5.6060E+08
12	2	6.08E−04	4.2267E−04	7.000E−04	0.0000	5.31E+07	3.6867E+07	6.0800E+07
12	3	5.51E−04	2.8249E−04	7.000E−04	0.0076	4.46E+07	2.2927E+07	5.2800E+07

Continued

12	4	8.97E−02	9.1622E−02	8.920E−02	0.1111	2.65E+09	2.7023E+09	2.6460E+09
12	5	1.59E−01	1.6943E−01	1.601E−01	0.1542	4.37E+09	4.6533E+09	4.4367E+09
13	2	1.24E−02	6.9183E−03	1.300E−02	----	1.31E+09	7.3167E+08	1.3680E+09
13	3	2.86E−04	5.2481E−05	4.000E−04	----	2.83E+07	5.1933E+06	3.5600E+07
13	4	1.96E−01	2.0417E−01	1.952E−01	0.2017	8.02E+09	8.3033E+09	7.9133E+09
13	5	9.70E−02	1.0139E−01	9.450E−02	0.1224	3.74E+09	3.8800E+09	3.6167E+09
14	2	1.78E−03	1.2823E−03	1.800E−03	----	1.16E+08	8.3220E+07	1.1690E+08
14	3	1.08E−03	1.2853E−03	1.000E−03	----	6.57E+07	7.8180E+07	6.2340E+07
14	5	5.08E−01	5.1642E−01	5.074E−01	0.5590	1.22E+10	1.2278E+10	1.2140E+10
15	3	5.19E−02	3.7154E−02	4.470E−02	----	2.14E+10	1.4450E+10	1.7370E+10
15	5	1.15E−01	1.0447E−01	1.125E−01	0.1002	2.19E+10	1.8200E+10	1.9640E+10
16	6	1.02E−01	1.1015E−01	9.950E−02	0.1190	1.80E+10	1.9500E+10	1.7480E+10
16	13	8.34E−04	7.3961E−04	8.000E−04	----	1.57E+07	1.4110E+07	1.5230E+07
17	1	9.08E−03	1.7539E−02	1.070E−02	----	2.37E+11	4.5833E+11	2.7840E+11
17	6	2.41E−01	2.5061E−01	2.368E−01	0.1374	1.50E+10	1.5670E+10	1.4670E+10
17	7	2.75E−02	3.1477E−02	2.580E−02	0.0416	1.53E+09	1.7543E+09	1.4320E+09
17	9	1.03E−03	2.2961E−03	1.400E−03	0.0578	4.56E+07	1.0280E+08	6.0967E+07
17	10	3.59E−02	3.9902E−02	3.570E−02	0.0095	1.40E+09	1.5723E+09	1.4040E+09
17	11	3.27E−03	5.1168E−03	3.300E−03	0.0551	7.69E+07	1.2400E+08	7.9167E+07
18	8	9.17E−01	2.3227E−02	1.880E−02	----	1.54E+10	7.1220E+08	3.1800E+08
19	6	1.78E−01	----	1.692E-01	0.1613	7.31E+09	----	3.8478E+09
19	7	7.27E−02	----	----	0.0483	2.69E+09	----	----
19	8	2.05E−02	9.4842E−01	9.122E−01	0.0245	6.25E+08	1.6189E+10	2.7820E+10
19	9	5.28E−02	----	----	0.0966	1.57E+09	----	----
19	10	1.94E−01	----	----	0.2101	5.12E+09	----	----
19	12	2.59E−04	----	----	----	2.58E+06	----	----
19	14	5.61E−04	----	----	----	3.02E+06	----	----
20	7	6.62E−01	6.8707E−01	6.600E−01	0.6821	1.76E+10	1.8343E+10	1.7643E+10
20	8	1.08E−01	8.6896E−02	1.058E−01	0.1138	2.37E+09	1.9229E+09	2.3443E+09
20	10	9.78E−03	2.7102E−02	1.010E−02	0.0087	1.86E+08	5.2129E+08	1.9514E+08
21	6	2.98E−02	5.4325E−02	3.670E−02	0.0597	1.34E+09	2.4340E+09	1.6360E+09
21	7	1.75E−01	2.0370E−01	----	0.2015	7.08E+09	8.2260E+09	7.3560E+09
21	8	6.42E−03	9.7051E−03	----	0.0118	2.16E+08	3.2740E+08	2.4860E+08
21	9	3.47E−01	3.0761E−01	----	0.3133	1.14E+10	1.0172E+10	1.0940E+10
21	10	6.08E−03	3.9355E−05	----	0.0005	1.78E+08	1.1614E+06	9.4940E+07
22	7	3.17E−03	2.3659E−04	----	0.1574	9.73E+07	7.2943E+06	8.9543E+07
22	8	1.51E−01	1.7219E−01	----	0.0045	3.87E+09	4.4671E+09	3.8886E+09
22	10	6.04E−01	5.9429E−01	----	0.6387	1.36E+10	1.3539E+10	1.3590E+10
23	1	1.21E+00	1.4060E+00	----	----	3.23E+13	3.7600E+13	3.2120E+13
23	9	1.59E−01	1.5560E−01	----	0.0691	1.19E+10	1.1437E+10	1.1690E+10
23	11	1.54E−01	1.5171E−01	----	0.0934	7.27E+09	7.0300E+09	7.1367E+09
24	6	4.29E−04	7.0469E−04	----	----	3.81E+07	6.1980E+07	4.5200E+07
24	7	7.98E−04	1.1561E−04	----	----	6.60E+07	9.4500E+06	6.1840E+07

Continued

24	10	3.70E−04	7.4473E−04	----	----	2.46E+07	4.9180E+07	3.8180E+07
24	12	4.79E−01	4.7643E−01	----	0.0191	1.83E+10	1.7818E+10	1.7880E+10
24	13	1.13E−02	1.6943E−05	----	----	3.34E+08	4.9140E+05	2.1240E+08
24	14	6.99E−02	9.1201E−02	----	0.0608	1.99E+09	2.5640E+09	2.0880E+09
25	6	9.36E−04	6.1235E−04	----	----	8.59E+07	5.5860E+07	6.6320E+07
25	7	2.24E−03	3.6141E−03	----	----	1.91E+08	3.0660E+08	2.0400E+08
25	8	3.72E−03	1.3428E−03	----	----	2.81E+08	1.0084E+08	3.4300E+08
25	9	1.27E−04	4.6345E−06	----	----	9.45E+06	3.4380E+05	1.2870E+07
25	10	8.28E−03	6.5615E−03	----	----	5.71E+08	4.5180E+08	6.4040E+08
25	12	2.48E−04	9.8628E−03	----	0.0028	9.91E+06	3.8980E+08	1.7430E+06
25	13	4.55E−01	4.7863E−01	----	0.4467	1.41E+10	1.4806E+10	1.4020E+10
25	14	5.15E−02	3.3651E−02	----	0.0653	1.55E+09	1.0066E+09	1.3530E+09
26	7	2.06E−04	4.4157E−05	----	----	1.29E+07	2.7300E+06	1.5157E+07
26	8	2.27E−03	2.3174E−03	----	----	1.26E+08	1.2674E+08	1.3200E+08
26	10	1.87E−04	7.6384E−04	----	----	9.45E+06	3.8286E+07	1.0320E+07
26	14	7.32E−01	7.4131E−01	----	0.7396	1.63E+10	1.6329E+10	1.6200E+10
27	1	2.14E+00	1.9861E+00	----	----	5.97E+13	5.5400E+13	5.9600E+13
27	12	1.11E−01	1.1041E−01	----	0.0948	9.62E+09	9.0600E+09	9.1033E+09
27	15	1.44E−01	1.5524E−01	----	0.1571	6.28E+09	6.9133E+09	6.8567E+09
28	2	3.12E−01	----	----	----	1.70E+11	----	9.3233E+10
28	3	7.53E−02	----	----	----	3.97E+10	----	2.1890E+10
28	4	5.48E−02	----	----	----	2.07E+10	----	1.0920E+10
28	5	9.63E−02	----	----	----	3.56E+10	----	1.8670E+10
29	3	7.57E−02	----	----	----	1.32E+11	----	6.7650E+10
29	5	3.91E−02	----	----	----	4.86E+10	----	2.1740E+10
29	23	2.05E−03	----	----	----	5.43E+08	----	1.3400E+08
29	27	3.36E−03	----	----	0.0003	3.38E+08	----	2.6180E+07
30	6	7.81E−02	----	----	----	1.30E+11	----	6.2310E+10
30	9	3.01E−02	----	----	----	4.51E+10	----	2.1320E+10
30	12	5.20E−02	----	----	----	5.86E+10	----	2.4570E+10
30	13	1.28E−03	----	----	----	1.31E+09	----	9.2910E+08
30	28	9.37E−02	----	----	0.0866	8.21E+09	----	4.9130E+09
31	1	6.68E−02	----	----	----	2.10E+12	----	1.6030E+12
31	6	4.63E−02	----	----	----	2.60E+10	----	1.2140E+10
31	7	2.89E−01	----	2.054E−01	----	1.56E+11	----	7.3700E+10
31	9	7.46E−04	----	1.200E−03	----	3.75E+08	----	3.9933E+08
31	10	4.70E−03	----	4.100E−03	----	2.28E+09	----	1.2790E+09
31	11	1.73E−02	----	1.140E−02	----	7.37E+09	----	3.0550E+09
31	12	9.38E−02	----	6.860E−02	----	3.56E+10	----	1.5760E+10
31	13	4.43E−03	----	3.700E−03	----	1.52E+09	----	7.5467E+08
31	14	2.32E−03	----	1.200E−03	----	7.86E+08	----	2.2760E+08
31	15	3.62E−02	----	3.250E−02	----	1.02E+10	----	5.3233E+09
31	28	2.35E−01	----	1.990E−01	0.2284	7.12E+09	----	4.3367E+09

Continued

31	29	3.84E−02	----	3.270E−02	----	7.34E+08	----	4.5700E+08
32	6	5.93E−03	----	2.600E−03	----	2.14E+09	----	6.4740E+08
32	7	1.59E−03	----	9.000E−04	----	5.54E+08	----	2.1140E+08
32	8	4.35E−01	----	3.034E−01	----	1.42E+11	----	6.6100E+10
32	9	2.05E−02	----	1.370E−02	----	6.65E+09	----	2.9480E+09
32	10	1.28E−01	----	9.580E−02	----	4.02E+10	----	1.9850E+10
32	12	9.76E−04	----	8.000E−04	----	2.41E+08	----	1.1380E+08
32	13	8.13E−02	----	5.510E−02	----	1.82E+10	----	7.4940E+09
32	14	1.20E−01	----	8.710E−02	----	2.65E+10	----	1.1660E+10
32	28	5.61E−01	----	4.884E−01	----	1.35E+10	----	8.8360E+09
33	1	2.94E−01	----	2.689E−01	----	9.37E+12	----	8.1633E+12
33	6	6.25E−03	----	4.300E−03	----	3.85E+09	----	1.7920E+09
33	7	6.11E−03	----	4.400E−03	----	3.63E+09	----	1.7370E+09
33	9	1.18E−01	----	8.710E−02	----	6.55E+10	----	3.2250E+10
33	10	1.36E−01	----	9.750E−02	----	7.27E+10	----	3.4667E+10
33	11	3.92E−02	----	3.350E−02	----	1.86E+10	----	1.0200E+10
33	12	8.19E−03	----	7.400E−03	----	3.48E+09	----	1.9470E+09
33	13	3.96E−02	----	3.140E−02	----	1.53E+10	----	7.3833E+09
33	14	1.19E−01	----	8.090E−02	----	4.54E+10	----	1.8700E+10
33	15	4.86E−02	----	3.990E−02	----	1.55E+10	----	7.6933E+09
33	28	6.38E−02	----	5.630E−02	0.0697	2.80E+09	----	1.8650E+09
33	29	2.21E−01	----	1.892E−01	0.2430	6.69E+09	----	4.4000E+09
34	16	2.63E−02	----	1.660E−02	----	1.46E+10	----	5.9533E+09
34	17	6.04E−02	----	3.970E−02	----	3.30E+10	----	1.3880E+10
34	19	3.26E−02	----	----	----	1.72E+10	----	----
34	21	1.13E−01	----	8.290E−02	----	5.80E+10	----	2.6690E+10
34	23	4.12E−02	----	2.970E−02	----	1.87E+10	----	8.2633E+09
34	24	1.09E−01	----	7.540E−02	----	3.97E+10	----	1.5690E+10
34	25	8.82E−04	----	2.000E−04	----	3.15E+08	----	5.5600E+07
34	27	1.63E−02	----	1.250E−02	----	5.13E+09	----	2.1360E+09
34	30	1.98E−01	----	1.875E−01	0.2028	1.16E+10	----	1.0040E+10
34	31	1.19E−01	----	1.107E−01	0.1190	6.80E+09	----	5.7400E+09
34	32	8.58E−03	----	8.000E−03	----	3.91E+08	----	3.2560E+08
34	33	2.28E−02	----	2.230E−02	0.0207	9.49E+08	----	8.3367E+08
35	17	2.53E−02	----	1.570E−02	----	8.32E+09	----	3.3160E+09
35	19	9.06E−02	----	----	----	2.88E+10	----	----
35	20	3.05E−01	----	2.106E−01	----	9.68E+10	----	4.2360E+10
35	21	5.55E−03	----	----	----	1.71E+09	----	9.6780E+08
35	22	3.89E−02	----	----	----	1.17E+10	----	5.5680E+09
35	23	3.11E−02	----	----	----	8.53E+09	----	3.4440E+09
35	24	7.59E−02	----	----	----	1.67E+10	----	6.0480E+09
35	25	3.18E−02	----	----	----	6.85E+09	----	3.3620E+09
35	26	4.46E−02	----	----	----	9.47E+09	----	3.8180E+09

Continued

35	27	2.23E−02	----	----	----	4.24E+09	----	1.1170E+09
35	31	3.98E−01	----	----	0.4009	1.39E+10	----	1.1860E+10
35	32	1.30E−01	----	----	----	3.60E+09	----	3.0320E+09
35	33	4.04E−02	----	----	0.0403	1.02E+09	----	9.4340E+08
36	18	5.29E−01	----	----	----	1.22E+11	----	2.4014E+09
36	19	2.52E−02	----	----	----	5.79E+09	----	5.4543E+10
36	20	5.20E−04	----	----	----	1.19E+08	----	7.0343E+07
36	21	1.27E−02	----	----	----	2.82E+09	----	1.0570E+09
36	22	1.65E−01	----	----	----	3.59E+10	----	1.5700E+10
36	24	1.53E−03	----	----	----	2.44E+08	----	7.1843E+07
36	25	8.08E−02	----	----	----	1.26E+10	----	3.9943E+09
36	26	1.33E−01	----	----	----	2.04E+10	----	7.9014E+09
36	32	7.51E−01	----	----	----	1.54E+10	----	1.3070E+10
37	3	6.24E−04	----	----	----	5.14E+08	----	2.8880E+08
37	5	5.56E−04	----	----	----	3.70E+08	----	2.3160E+08
37	17	1.26E−03	----	----	----	4.51E+08	----	2.2120E+08
37	19	2.48E−02	----	----	----	8.57E+09	----	----
37	20	1.04E−01	----	----	----	3.58E+10	----	1.7050E+10
37	21	1.20E−01	----	----	----	4.03E+10	----	1.7640E+10
37	22	1.48E−01	----	----	----	4.87E+10	----	2.1580E+10
37	23	3.73E−02	----	----	----	1.12E+10	----	4.3680E+09
37	24	3.98E−02	----	----	----	9.64E+09	----	4.2460E+09
37	25	4.45E−02	----	----	----	1.06E+10	----	3.8760E+09
37	26	1.42E−01	----	----	----	3.34E+10	----	1.3290E+10
37	27	3.24E−02	----	----	----	6.84E+09	----	1.6950E+09
37	31	8.53E−02	----	----	0.0855	3.78E+09	----	3.5220E+09
37	32	1.24E−03	----	----	0.0019	4.49E+07	----	2.9640E+07
37	33	5.14E−01	----	----	0.5069	1.72E+10	----	1.4760E+10
38	6	1.56E−01	1.6368E−01	----	----	2.09E+11	2.2080E+11	----
38	7	1.23E−01	1.3274E−01	----	----	1.62E+11	1.7580E+11	----
38	8	3.78E−01	3.8548E−01	----	----	4.83E+11	4.9520E+11	----
38	10	1.55E−01	1.4859E−01	----	----	1.94E+11	1.8694E+11	----
38	12	1.32E−04	1.7701E−04	----	----	1.47E+08	1.9826E+08	----
38	13	3.36E−03	3.0130E−03	----	----	3.57E+09	3.2240E+09	----
38	14	9.20E−04	5.7810E−04	----	----	9.74E+08	6.1580E+08	----

i and j: The lower (i) and upper (j) levels of a transition as defined in Table 4. **gf (nm) (FAC)**: Weighted oscillator strengths from the FAC code (our calculation). **gf (nm) (COWAN)**: Weighted oscillator strengths from the COWAN code (also calculation). **gf (nm) (CIV3)**: Weighted oscillator strengths from the CIV3 code [22]. **gf (nm) (RCI)**: Weighted oscillator strengths from the RCI code [23]. **A_{ji} (s^{-1}) (FAC)**: Transition probabilities (in nm) from the FAC code (our calculation). **A_{ji} (s^{-1}) (COWAN)**: Transition probabilities (in nm) from the COWAN code (also calculation). **A_{ji} (s^{-1}) (CIV3)**: Transition probabilities (in nm) from the CIV3 code [22].

2. Gain Coefficient Computations

The possibility of laser emission from plasma of Ge XXIII ion via electron collisional pumping, in the XUV and soft X-ray spectral regions is investigated at different plasma temperatures and plasma electron densities. The reduced population densities are calculated by solving the coupled rate equations [13] [14].

$$N_j\left[\sum_{i<j}A_{ji}+N_e\left(\sum_{i<j}C_{ji}^d+\sum_{i>j}C_{ji}^e\right)\right]=N_e\left(\sum_{i<j}N_iC_{ij}^e+\sum_{i>j}N_iC_{ij}^d\right)+\sum_{i>j}N_iA_{ij} \quad (1)$$

where N_j and N_i is the fractional population of level j and i respectively, N_e is the electron density, A_{ji} is the Einstein coefficient for spontaneous radiative decay from *j* to *i*; and C_{ij}^e and C_{ji}^d represent the rate coefficient for collisional excitation and de-excitation respectively. The actual population density N_J of the j^{th} level can be calculated from the equation of identity [15] [16].

$$C_{ji}^d=C_{ij}^e\left[\frac{g_i}{g_j}\right]\exp\left[\frac{\Delta E_{ji}}{kT_e}\right] \quad (2)$$

where g_i and g_j are the statistical weights of the lower and upper levels, respectively.

The electron impact excitation rates usually are expressed via the effective collision strengths γ_{ji} as

$$C_{ji}^d=\frac{8.6287\times10^{-6}}{g_jT_e^{1/2}}\gamma_{ij} \quad (3)$$

where the values of γ_{ji} and A_{ji} are obtained by [17].

The actual population density N_J of the j^{th} level is obtained from the following identity [17],

$$N_J=N_j\times N_i \quad (4)$$

where N_I is the quantity of ions which reached to the ionization stage *I* [17],

$$N_I=f_I\,N_e/Z_{avg} \quad (5)$$

where N_e is the electron density, Z_{avg} is the average degree of ionization and f_I is the fractional abundance of the ionization states which can be calculated from the relation [17]. Since the populations calculated from Equation (1) are normalized such that,

$$\sum_{J=1}^{241}\frac{N_J}{N_I}=1 \quad (6)$$

where 241 is the number of all the levels of the ion under consideration, the quantity actually obtained from Equation (1) is the fractional population N_J/N_I. After the calculation of levels population, the quantities N_j/g_j and N_i/g_i can be calculated. Application of electron collisional pumping, the collision in the laser ion plasma will transfer the pumped quanta to other levels, and will result in population inversions between the upper and lower levels. Once a population inversion has been ensured a positive gain through $F>0$ [18] is obtained.

$$F=\frac{g_j}{N_j}\left[\frac{N_j}{g_j}-\frac{N_i}{g_i}\right] \quad (7)$$

where N_j/g_j and N_i/g_i are the reduced populations of the upper level and lower level respectively. Equation (7) has been used to calculate the gain coefficient (α) for Doppler broadening of the various transitions in the Ge XXIII ion.

$$\alpha_{ji}=\frac{\lambda_{ij}^3}{8\pi}\left[\frac{M}{2\pi KT_i}\right]^{1/2}A_{ji}N_jF \quad (8)$$

where *M* is the ion mass λ_{ij} is the transition wavelength in cm (see **Table 3**), T_i is the ion temperature in K and j, I represents the upper and lower transition levels respectively.

As seen from Equation (8), the gain coefficient is expressed in terms of the upper state density (N_j). This quantity N_j depends on how the upper state is populated, as well as on the density of the initial source state. The source state is often the ground state for the particular ion.

3. Results and Discussions

3.1. Energy Levels

The energy level values obtained using the fully relativistic flexible atomic code (FAC) for the $1s^2\,2s^2\,2p^5nl$, $1s^2$

Table 3. Comparison between some wavelengths (λ) for E1 transitions of Ge XXIII (in nm).

j	i	λ (nm) (FAC)	λ (nm) (COWAN)	λ (nm) (CIV3)	λ (nm) (MCDF)	λ (nm) (RCI)	λ (nm) (Exp.)
3	1	1.00291911	1.0009	1.001	----	----	----
5	1	0.978298138	0.9763	0.976	----	----	----
6	2	29.06054601	29.0804	29.1	----	----	----
7	2	26.82759761	26.7880	26.85	----	----	----
7	3	28.60854399	28.5017	28.48	28.644	28.432	28.628
8	2	23.76385089	23.7695	23.82	23.760	24.192	23.767
9	2	23.38618832	23.5053	23.51	23.395	24.151	23.385
9	3	24.72809857	24.8145	24.75	24.727	25.422	24.735
10	2	22.00458606	22.0738	22.16	----	----	----
10	3	23.18861213	23.2245	23.26	23.229	24.033	23.224
10	5	55.46243419	56.1774	56.06	----	----	----
11	3	19.06599826	19.1780	19.09	----	----	----
11	5	36.55639248	37.1945	36.72	----	----	----
12	2	15.97797365	15.9610	15.98	----	----	----
12	3	16.59318561	16.5540	16.54	----	----	----
12	4	27.43670009	27.4431	27.39	----	----	----
12	5	28.43226568	28.4487	28.32	28.475	28.318	28.509
13	2	14.48681287	14.4972	14.54	----	----	----
13	3	14.99074178	14.9848	15	----	----	----
13	4	23.31563846	23.3836	23.42	23.319	23.390	23.314
13	5	24.03069931	24.1098	24.1	24.044	23.900	24.049
14	2	14.32320141	14.3395	14.36	----	----	----
14	3	14.81561859	14.8164	14.81	----	----	----
14	5	23.58382453	23.6768	23.61	23.627	23.407	23.625
15	3	12.74125872	13.0918	13.1	----	----	----
15	5	18.72982602	19.5593	19.55	19.544	19.399	19.619
16	6	19.4465226	19.4149	19.49	19.399	19.701	19.460
16	13	59.50360748	59.1173	59.16	----	----	----
17	1	0.924189369	0.9223	0.922	----	----	----
17	6	18.92164195	18.8596	18.94	18.878	19.045	18.940
17	7	20.00584033	19.9678	20.03	----	----	----
17	9	22.47182417	22.2880	22.41	----	----	----
17	10	23.91464589	23.7483	23.78	----	----	----
17	11	30.77812808	30.2817	30.63	----	----	----
18	8	20.99113251	20.8451	20.93	----	----	----
19	6	18.02121903	----	18.05	----	----	----
19	7	19.00201092	----	----	18.895	18.877	18.961
19	8	20.91160561	20.8281	20.91	----	----	----
19	9	21.21305773	----	----	----	----	----
19	10	22.49415888	----	----	----	----	----
19	12	36.61005733	----	----	----	----	----
19	14	49.79022451	----	----	----	----	----

Continued

20	7	18.94688793	18.9013	18.88	18.814	18.874	18.880
20	8	20.84486629	20.7616	20.74	----	----	----
20	10	22.4169586	22.2548	22.18	----	----	----
21	6	17.27924434	17.2601	17.3	----	----	----
21	7	18.17892	18.1837	18.2	----	----	----
21	8	19.9190906	19.8990	19.92	19.814	19.669	19.873
21	9	20.1924195	20.0880	20.14	----	----	----
21	10	21.3498462	21.2667	21.25	----	----	----
22	7	17.6454186	17.5769	17.67	----	----	----
22	8	19.2803566	19.1747	19.29	19.192	18.936	19.259
22	10	20.617748	20.4414	20.53	20.475	19.815	20.539
23	1	0.91269295	0.9117	0.911	----	----	----
23	9	17.2029364	17.3848	17.21	----	----	----
23	11	21.6825457	21.8925	21.67	----	----	----
24	6	12.2585873	12.3094	12.28	----	----	----
24	7	12.704653	12.7720	12.73	----	----	----
24	10	14.1760934	14.2199	14.14	----	----	----
24	12	18.7265184	18.8773	18.79	----	----	----
24	13	21.295593	21.4373	21.26	----	----	----
24	14	21.6592895	21.7917	21.65	----	----	----
25	6	12.0678472	12.0887	12.1	----	----	----
25	7	12.4998937	12.5346	12.54	----	----	----
25	8	13.2987553	13.3265	13.33	----	----	----
25	9	13.4200377	13.4110	13.43	----	----	----
25	10	13.921634	13.9263	13.91	----	----	----
25	12	18.285025	18.3634	18.38	----	----	----
25	13	20.7264947	20.7769	20.74	----	----	----
25	14	21.0708515	21.1096	21.11	----	----	----
26	7	12.3577809	12.4198	12.38	----	----	----
26	8	13.138017	13.1968	13.15	----	----	----
26	10	13.7455841	13.7847	13.71	----	----	----
26	14	20.6701616	20.7860	20.65	20.519	20.644	20.583
27	1	0.89303659	0.8927	0.892	----	----	----
27	12	16.0204352	16.4624	16.1	----	----	----
27	15	22.6240255	22.3370	21.61	----	----	----
28	2	6.39977902	----	7.52	----	----	----
28	3	6.49625131	----	7.64	----	----	----
28	4	7.68540454	----	9.36	----	----	----
28	5	7.76153141	----	9.46	----	----	----
29	3	6.19256802	----	7.29	----	----	----
29	5	7.33194183	----	8.93	----	----	----
29	23	15.8945958	----	25.93	----	----	----
29	27	25.774576	----	68.98	----	----	----

Continued

30	6	6.32686538	----	7.74	----	----	----
30	9	6.67972533	----	8.27	----	----	----
30	12	7.69935951	----	9.91	----	----	----
30	13	8.10118282	----	10.56	----	----	----
30	28	27.6154168	----	32.75	----	----	----
31	1	0.84183128	----	0.861	----	----	----
31	6	6.30092271	----	7.7	----	----	----
31	7	6.416725578	----	7.87	----	----	----
31	9	6.650814849	----	8.21	----	----	----
31	10	6.77173044	----	8.39	----	----	----
31	11	7.228153142	----	9.11	----	----	----
31	12	7.660979329	----	9.83	----	----	----
31	13	8.058697858	----	10.47	----	----	----
31	14	8.110232992	----	10.57	----	----	----
31	15	8.903756621	----	11.65	----	----	----
31	28	27.1279177	----	31.94	----	----	----
31	29	34.1140454	----	39.92	----	----	----
32	6	6.089149806	----	7.38	----	----	----
32	7	6.197229399	----	7.54	----	----	----
32	8	6.387459838	----	7.82	----	----	----
32	9	6.415305514	----	7.86	----	----	----
32	10	6.527736953	----	8.02	----	----	----
32	12	7.35016756	----	9.33	----	----	----
32	13	7.715504567	----	9.9	----	----	----
32	14	7.762726026	----	9.98	----	----	----
32	28	23.59488012	----	27.15	----	----	----
33	1	0.836515264	----	0.856	----	----	----
33	6	6.014819126	----	7.29	----	----	----
33	7	6.120253309	----	7.44	----	----	----
33	9	6.33285591	----	7.75	----	----	----
33	10	6.442391307	----	7.91	----	----	----
33	11	6.854144356	----	8.54	----	----	----
33	12	7.242135475	----	9.18	----	----	----
33	13	7.596553105	----	9.73	----	----	----
33	14	7.642330131	----	9.81	----	----	----
33	15	8.342972988	----	10.74	----	----	----
33	28	22.51667288	----	25.91	----	----	----
33	29	27.12777534	----	30.91	----	----	----
34	16	6.32759139	----	7.88	----	----	----
34	17	6.385224484	----	7.97	----	----	----
34	19	6.494731238	----	----	----	----	----
34	21	6.596819889	----	8.31	----	----	----
34	23	6.993883236	----	8.94	----	----	----

Continued

34	24	7.819488144	----	10.34	----	----	----
34	25	7.89912776	----	10.46	----	----	----
34	27	8.412867128	----	11.38	----	----	----
34	30	19.45339221	----	20.38	----	19.340	19.209
34	31	19.70280794	----	20.71	----	----	----
34	32	22.10702133	----	23.38	----	----	----
34	33	23.14544859	----	24.39	----	----	----
35	17	6.370709831	----	7.95	----	----	----
35	19	6.479715048	----	----	----	----	----
35	20	6.486151251	----	8.144	----	----	----
35	21	6.58132848	----	8.28	----	----	----
35	22	6.65416425	----	8.393	----	----	----
35	23	6.97647331	----	8.9	----	----	----
35	24	7.79773163	----	10.29	----	----	----
35	25	7.87692645	----	10.42	----	----	----
35	26	7.93442318	----	10.53	----	----	----
35	27	8.38768868	----	11.33	----	----	----
35	31	19.5652593	----	20.52	----	19.544	19.414
35	32	21.9340035	----	23.15	----	----	----
35	33	22.9558645	----	24.14	----	----	----
36	18	6.44169557	----	8.07	----	----	----
36	19	6.44922283	----	8.07	----	----	----
36	20	6.45559522	----	8.096	----	----	----
36	21	6.54987129	----	8.23	----	----	----
36	22	6.62200863	----	8.342	----	----	----
36	24	7.75361057	----	10.21	----	----	----
36	25	7.83190723	----	10.34	----	----	----
36	26	7.88874624	----	10.45	----	----	----
36	32	21.5884556	----	22.76	----	----	----
37	3	4.02622122	----	4.6	----	----	----
37	5	4.47873387	----	5.21	----	----	----
37	17	6.11875924	----	7.57	----	----	----
37	19	6.21924501	----	----	----	----	----
37	20	6.22517394	----	7.745	----	----	----
37	21	6.3127944	----	7.87	----	----	----
37	22	6.37977744	----	7.969	----	----	----
37	23	6.6754629	----	8.43	----	----	----
37	24	7.42357701	----	9.66	----	----	----
37	25	7.4953238	----	9.77	----	----	----
37	26	7.54736614	----	9.87	----	----	----
37	27	7.95634814	----	10.57	----	----	----
37	31	17.3688062	----	18.16	----	----	----
37	32	19.2105275	----	20.19	----	----	----

Continued

37	33	19.9898721	----	20.94	----	19.959	19.925
38	6	3.15614026	3.1459	----	----	----	----
38	7	3.18493053	3.1753	----	----	----	----
38	8	3.23443596	3.2238	----	----	----	----
38	10	3.27002	3.2577	----	----	----	----
38	12	3.46419347	3.4529	----	----	----	----
38	13	3.5432683	3.5300	----	----	----	----
38	14	3.55319554	3.5395	----	----	----	----

i and j: The lower (i) and upper (j) levels of a transition as defined in **Table 4**. **λ (nm) (FAC)**: Transition wavelengths (in nm) from the FAC code (our calculation). **λ (nm)(COWAN)**: Transition wavelengths (in nm) from the COWAN code (also calculation). **λ (nm) (CIV3)**: Transition wavelengths (in nm) from the CIV3 code [22]. **λ (nm) (MCDF)**: Transition wavelengths (in nm) from the MCDF code [23]. **λ (nm) (RCI)**: Transition wavelengths (in nm) from the RCI code [23]. **λ (nm) (Exp.)**: Transition wavelengths (in nm) calculated experimentally [23].

$2s^1\ 2p^6nl$ (n = 3, 4, 5, 6; l = s, p, d, f, g and h) configurations in Ne-like Ge ions are presented in **Table 1**. The main components of the computed Eigen vectors are also given in these tables in the jj-coupling schemes. For Ge XXIII, the agreement between FAC, MCDF, and other theoretical and experimental energies [19]-[23] with the values available at the National Institute of Standards and Technology (NIST) [24] and is within values less than 0.5% for a majority of levels.

3.2. Radiative Decay Rates

The oscillator strengths $\left(f_{ij}\right)$ and radiative rates $\left(A_{ij}\right)$ (in s^{-1}) for a transition $i \rightarrow j$ are related by the following expression

$$f_{ij} = \frac{mc}{8\pi^2 e^2}\lambda_{ij}^2\frac{\omega_j}{\omega_i}A_{ji} = 1.49\times10^{-16}\lambda_{ij}^2\frac{\omega_j}{\omega_i}A_{ji}$$

where m and e are the electron mass and charge, respectively, c is the velocity of light, λ_{ij} is the transition wavelength in Å and ω_i and ω_j are the statistical weights of the lower i and upper j levels, respectively. Similarly, the oscillator strength $\left(f_{ij}\right)$

(Dimensionless) and the line strength S (in atomic units, $1\text{ a. u.} = 6.46\times10^{-36}\ \text{cm}^2\cdot\text{eus}^2$) are related by the following standard equations. For the electric dipole (E1) transitions,

$$A_{ji} = \frac{2.0261\times10^{18}}{\omega_j\lambda_{ij}^3}S^{E1} \quad\text{and}\quad f_{ij} = \frac{303.75}{\omega_j\lambda_{ij}^3}S^{E1}$$

The wavelengths, transition probabilities, and weighted oscillator strengths, for E1transitions calculated using the (FAC) are reported in **Table 2** and **Table 3** for Ge XXIII. We present a comparison between our results and other theoretical transition probabilities for allowed E1 transitions for Ge XXIII in tables respectively. It shows that our results are in a good agreement with the other theoretical and experimental results [22] [23]. **Table 2** shows a comparison between the FAC, MCDF, RCI, and other theoretical weighted oscillator strength [22] [23] values for some transitions among the levels of the $1s^2\ 2s^2\ 2p^5nl$, $1s^2\ 2s^1\ 2p^6nl$ (n = 3, 4, 5, 6; l = s, p, d, f, g and h) configurations for Ge XXIII. Generally, there are no discrepancies between our FAC, COWAN, CIV3, MCDF, RCI, and experimental calculations and the agreement is within ≤20% for strong transitions.

3.3. Level Population

The reduced population densities are calculated for 241 finestructure levels arising from $1s^2\ 2s^2\ 2p^6nl$, $1s^2\ 2s^2\ 2p^5\ nl$, $1s^2\ 2s^1\ 2p^6\ nl$ (n = 3, 4, 5, 6; l = s, p, d, f, g and h) configurations that emit radiation in the XUV and soft X-ray spectral regions. The calculations were performed by solving the coupled rate Equation (1) simultaneously using MATLAB R2013acomputer program. The present calculations for the reduced populations as a function of electron densities are plotted in **Figure 1** to **Figure 4** for levels (5, 15, 33, 37) of the configurations $[(2p_{1\backslash2}3s_{1\backslash2})_1, (2p_{1\backslash2}3p_{1\backslash2})_0, (2s_{1\backslash2}3p_{1\backslash2})_1, (2s_{1\backslash2}3d_{5\backslash2})_2]$ at different plasma temperatures (650, 850, 1050, 1250, 1450,

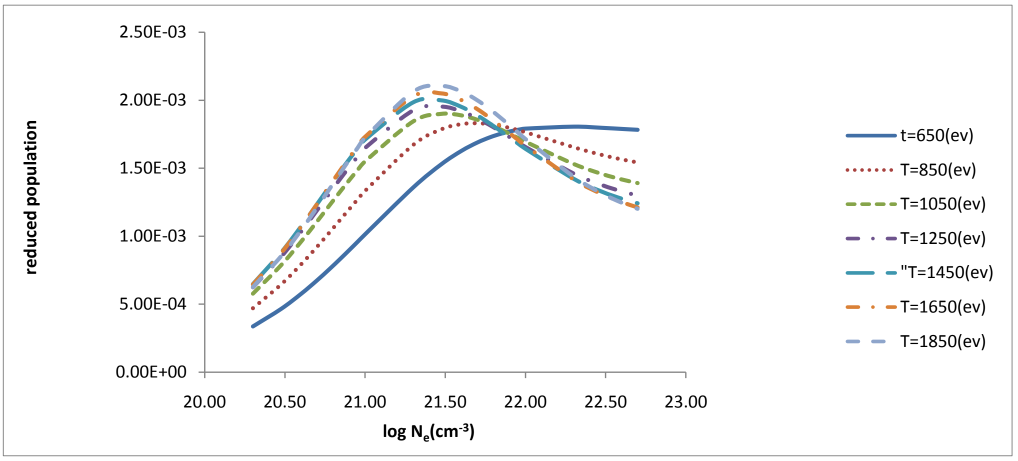

Figure 1. Reduced population of level $(2p_{1\backslash 2}3s_{1\backslash 2})_1$ for Ge XXIII after electron collisional pumping as a function of the electron density at temperatures (650, 850, 1050, 1250, 1450, 1650, and 1850) eV.

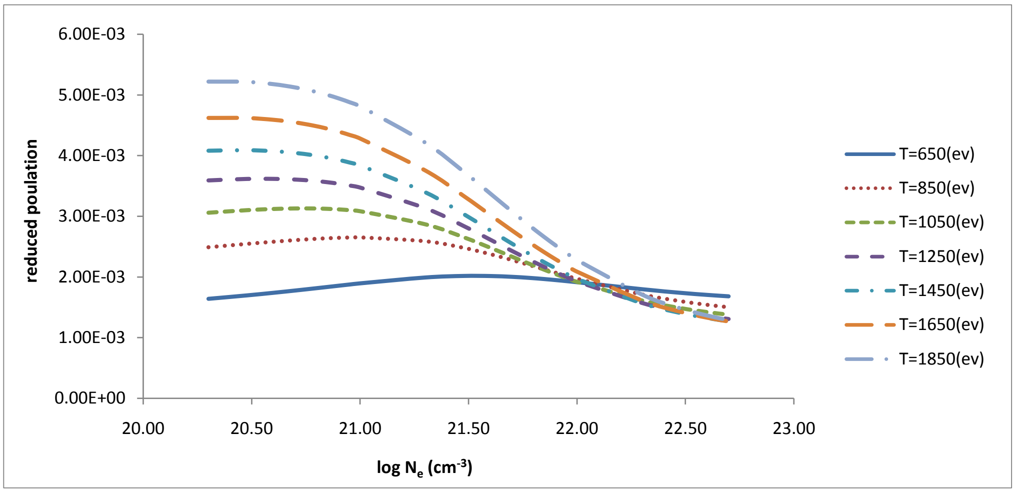

Figure 2. Reduced population of level $(2p_{1\backslash 2}3p_{1\backslash 2})_0$ for Ge XXIII after electron collisional pumping as a function of the electron density at temperatures (650, 850, 1050, 1250, 1450, 1650, and 1850) eV.

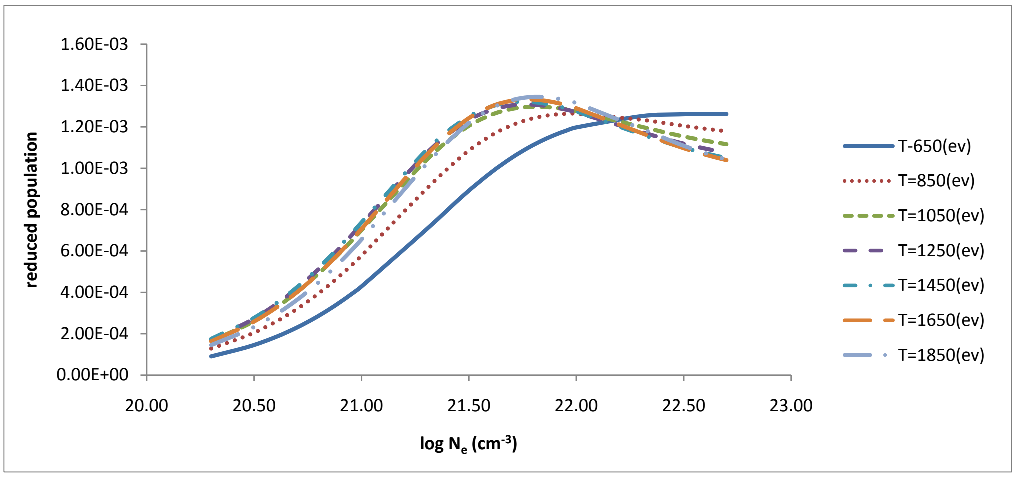

Figure 3. Reduced population of level $(2s_{1\backslash 2}3p_{1\backslash 2})_1$ for Ge XXIII after electron collisional pumping as a function of the electron density at temperatures (650, 850, 1050, 1250, 1450, 1650, and 1850) eV.

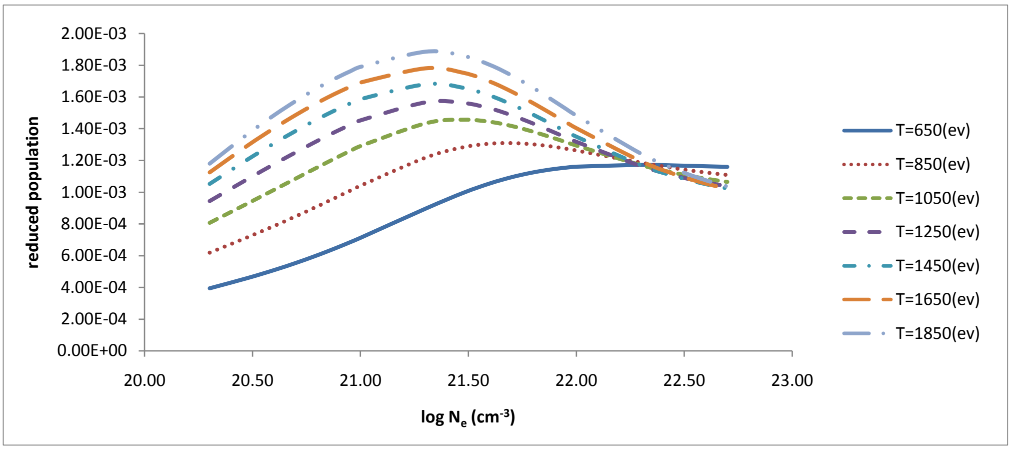

Figure 4. Reduced population of level $(2s_{1\backslash 2}3d_{5\backslash 2})_2$ for Ge XXIII after electron collisional pumping as a function of the electron density at temperatures (650, 850, 1050, 1250, 1450, 1650, and 1850) eV.

1650, and 1850) eV for Ge XXIII ion. In the calculation we took into account spontaneous radiative decay rate and electron collisional processes between all levels under the study. The behavior of level populations of the various ions can be explained as follows: in general at low electron densities the reduced population density is proportional to the electron density, where excitation to an excited state is followed immediately by radiative decay, and collisional mixing of excited levels can be ignored. This result is in agreement with that of Feldman *et al*. [19]-[21]. At high electron densities (Ne > 5 × 10^{22}), the radiative decay to all the levels will be negligible compared to collisional depopulations and all the level populations become independent of the electron density and are approximately equal (see **Figures 1** to **4**).

3.4. Radiative Lifetime

The lifetimes are determined almost entirely from the allowed and the strong inter combination transitions. The radiative lifetime τ_j of an excited atomic state *j*, is related to the atomic transition probability A_{ji} by:

$$\tau_j = \frac{1}{\sum_i A_{ji}} \tag{9}$$

where the sum is extended over all the lower states which can be reached from the upper state by radiative decay.

Table 4 contains the present results of radiative lifetime for the upper and lower laser levels for the Ge XXIII.

3.5. Inversion Factor

As we mentioned before, laser amplification will occur only if there is population inversion, or in other words, for positive inversion factor F > 0. However, large amplification, the gain exceeds all losses and ensures laser emission. In order to work in the XUV and X-ray spectral regions, we have selected transitions between any two levels producing photons with wavelengths between 12 and 52 nm. The electron density at which the population reaches corona equilibrium approximately equals to A/D, where A is the radiative decay rate and D is the collisional de-excitation rate [19] [21]. The population in version is largest where the electron collisions de-excitation rate for the upper level is comparable to the radiative decay rate for this level.

3.6. Gain Coefficient

As a result of population inversion there will be positive gain in laser medium. Equation (8) has been used to calculate gain coefficient for the Doppler broadening of various transitions in the Ge XXIII ion. Our results for the maximum gain coefficient in cm^{-1} for those transitions having appositive inversion factor F > 0 in the case of Ge XXIII ion at different temperatures are calculated (see **Table 4**) and plotted against electron density in **Figure 5** and **Figure 6**. The figures show that the population inversions occur for several transitions in the Ge

Table 4. Laser transitions, wavelength, radiative life time of the upper and lower laser levels in the possible laser transitions and maximum gain coefficient at temperatures (650, 850, 1050, 1250, 1450, 1650, and 1850) eV in the possible laser transitions.

Transition	Configuration	λ (nm)	τ_j (sec)	τ_j (sec)	Gain (α) (cm^{-1})						
					T = 650 (ev)	T = 850 (ev)	T = 1050 (ev)	T = 1250 (ev)	T = 1450 (ev)	T = 1650 (ev)	T = 1850 (ev)
7<>3	$(2p_{3\backslash2}3p_{1\backslash2})_2$-----$(2p_{3\backslash2}3s_{1\backslash2})_1$	28.609	1.34E−10	3.50E−13	7.5414	11.642	12.694	15.1191	17.125	21.4424	27.3609
9<>3	$(2p_{3\backslash2}3p_{3\backslash2})_1$-----$(2p_{3\backslash2}3s_{1\backslash2})_1$	24.728	9.66E−11	3.50E−13	1.8221	3.3047	3.98416	5.1061	6.12157	7.73807	9.7982
10<>3	$(2p_{3\backslash2}3p_{3\backslash2})_2$-----$(2p_{3\backslash2}3s_{1\backslash2})_1$	23.189	7.00E−11	3.50E−13	6.9387	10.867	11.8141	14.2795	16.3407	20.1334	26.2206
15<>3	$(2p_{1\backslash2}3p_{1\backslash2})_0$-----$(2p_{3\backslash2}3s_{1\backslash2})_1$	12.741	2.31E−11	3.50E−13	6.2797	8.4190	8.36027	9.22122	10.2872	12.461	15.8628
14<>5	$(2p_{1\backslash2}3p_{3\backslash2})_2$-----$(2p_{1\backslash2}3s_{1\backslash2})_1$	23.584	8.07E−11	4.84E−13	4.3045	7.6260	8.65851	11.4741	13.9279	17.4553	21.512
15<>5	$(2p_{1\backslash2}3p_{1\backslash2})_0$-----$(2p_{1\backslash2}3s_{1\backslash2})_1$	18.730	2.31E−11	4.84E−13	23.865	29.814	28.6124	30.9059	33.8385	40.33	50.4729
21<>9	$(2p_{3\backslash2}3d_{3\backslash2})_2$-----$(2p_{3\backslash2}3p_{3\backslash2})_1$	20.192	4.96E−11	9.66E−11	1.1868	2.415	2.95213	3.98613	5.01531	6.66205	9.3533
35<>31	$(2s_{1\backslash2}3d_{3\backslash2})_2$-----$(2s_{1\backslash2}3p_{1\backslash2})_1$	19.565	4.72E−12	4.26E−13	0.7458	1.7933	2.7096	3.52883	4.33676	5.74496	7.30669
37<>31	$(2s_{1\backslash2}3d_{5\backslash2})_2$-----$(2s_{1\backslash2}3p_{1\backslash2})_1$	17.369	4.40E−12	4.26E−13	1.7522	2.6849	3.21201	3.9254	4.57372	5.37767	6.34003
37<>33	$(2s_{1\backslash2}3d_{5\backslash2})_2$-----$(2s_{1\backslash2}3p_{3\backslash2})_1$	19.990	4.40E−12	1.04E−13	27.958	41.249	37.1457	53.8662	61.1486	72.0261	87.8871
45<>39	$(2p_{3\backslash2}4p_{3\backslash2})_0$-----$(2p_{3\backslash2}4s_{1\backslash2})_1$	45.130	1.09E−12	5.01E−13	1.3883	1.9549	2.4693	3.56572	4.27755	4.85807	5.29178
123<>96	$(2s_{1\backslash2}4d_{3\backslash2})_2$-----$(2s_{1\backslash2}4p_{3\backslash2})_1$	51.643	4.96E−13	6.92E−14	1.787	4.3711	5.82193	7.66273	9.93204	13.4196	18.2148

where τ_j is the radiative life time of the upper laser level; τ_j is the radiative life time of the lower laser level; λ is the laser transition wavelength in (nm); α is the gain coefficient in cm^{-1}.

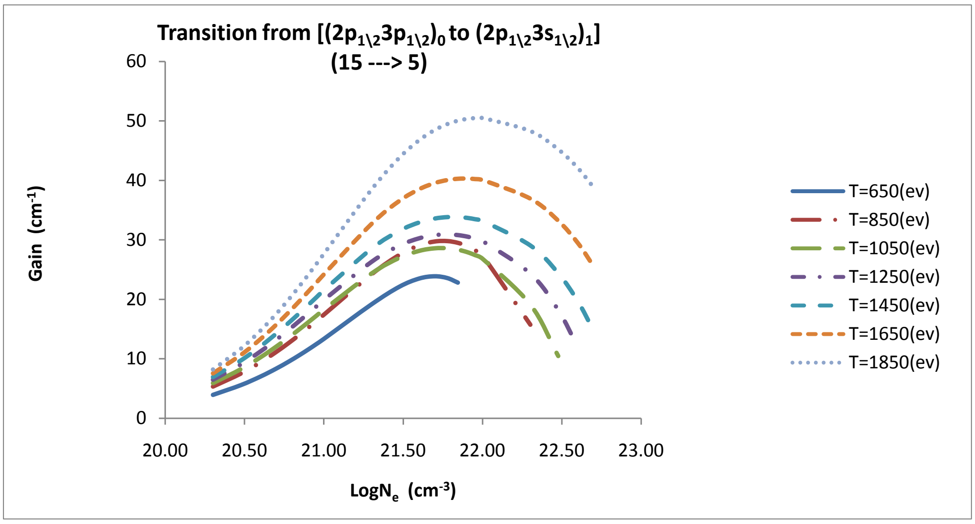

Figure 5. Gain coefficient against electron density (Ne) at different temperatures (650, 850, 1050, 1250, 1450, 1650, 1850) eV.

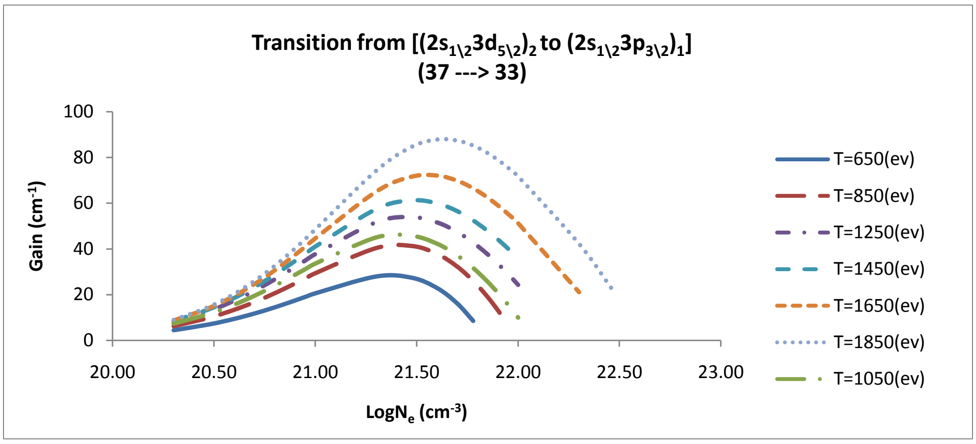

Figure 6. Gain coefficient against electron density (Ne) at different temperatures (650, 850, 1050, 1250, 1450, 1650, 1850) eV.

XXIII ion, however, the largest gain occurs for the Ge XXIII ion at $(2s_{1\backslash 2}3d_{5\backslash 2})_2$-----$(2s_{1\backslash 2}3p_{3\backslash 2})_1$ transition. These short wavelength laser transitions can be produced using plasmas created by optical lasers as the lasing medium. For Ge XXIII ion the rates for electron collisional excitation from the $1s^2\ 2s^2\ 2p^6$ ground state to the $1s^22s^12p^63d$ configuration are greater than the rates for excitation from the ground state to the $1s^22s^12p^63p$ state. For electron densities and electron temperatures that are typical of laboratory high-density plasma sources, such as laser produced plasmas, it is possible to create a quasi-stationary population inversion between the $2s^1\ 2p^63d$ and $2s^1\ 2p^63p$ states in Ge XXIII ion. Our calculations have shown that under favorable conditions large laser gains for this transition in the XUV and soft X-ray regions of the spectrum can be achieved in the Ge XXIII. The gain calculations were performed at electron temperatures equal to (650, 850, 1050, 1250, 1450, 1650, and 1850) eV at different electron densities. It is obvious that the gain increases with the temperature. We also find that some wavelengths for the lasing transitions in Table 4 are much closed to the values of it in the ref. [23] which give us the accurate wavelength calculated experimentally, although we Ignores some physical processes in the our rate equation.

4. Conclusions

The analysis of how the electron collisional pumping (ECP) is suitable for attaining population inversion and offering the potential for laser emission in the spectral region between 12 and 53 nm from the Ge XXIII ion.

This class of lasers can be achieved under the suitable conditions of pumping power as well as electron density. If the positive gains obtained previously for some transitions in the ions under studies (Ge XXIII ion) together with the calculated parameters can be achieved experimentally, then successful low-cost electron collisional pumping XUV and soft X-ray lasers can be developed for various applications. The results have suggested the laser transitions in the Ge XXIII plasma ion (see **Table 4**), as the most promising laser emission lines in the XUV and soft X-ray spectral regions.

References

[1] Gudzenko, L.I. and Shelepin, L.A. (1966) Amplification of Radiation in the Decay of a Maximally Ionized Plasma. *Journal of Applied Mechanics and Technical Physics*, **7**, 82.

[2] Maxon, S., Hagelstein, P., Reed, K. and Scofield, J. (1985) A Gas Puff Soft X-Ray Laser Target Design. *Journal of Applied Physics*, **57**, 971. http://dx.doi.org/10.1063/1.334700

[3] Vinogradov, A.V., Sobelman, I. and Yukov, E. (1977) Population Inversion of Transitions in Neon-Like Ions. *Soviet Journal of Quantum Electronics*, **7**, 32. http://dx.doi.org/10.1070/QE1977v007n01ABEH008807

[4] King, R.E., Pert, G.J., McCabe, S.P., Simms, P.A., MacPhee, A.G., Lewis, C.L.S., *et al*. (2001) Saturated X-Ray Lasers at 196 A and 73 A Pumped by Picosecond Travelling Wave Excitation. *Physical Review A*, **64**, Article ID: 053810. http://dx.doi.org/10.1103/PhysRevA.64.053810

[5] Rocca, J.J., Shlyaptsev, V., Tomasel, F.G., Cortázar, O.D., Hartshorn, D. and Chilla, J.L.A. (1994) Demonstration of a Discharge Pumped Table Top Soft X-Ray Laser. *Physical Review Letters*, **73**, 2192. http://dx.doi.org/10.1103/PhysRevLett.73.2192

[6] Tomsel, F.G., Rocca, J.J., Shlyaptsev, V.N. and Macchietto, C.D. (1997) Lasing at 60.8 nm in Ne-Like Sulfur Ions in Ablated Material Excited by a Capillary Discharge. *Physical Review A*, **55**, 1437.

[7] Healy, S.P., Janulewicz, K.A. and Pert, G.J. (1997) Short Wavelength Lasing on Collisionally Pumped, Highly Excited 2s Hole States of Neon Like Ions in Performed Plasmas Irradiated with Picosecond Pulses. *Optics Communications*, **144**, 24-30. http://dx.doi.org/10.1016/S0030-4018(97)00287-3

[8] Simms, P.A., McCabe, S. and Pert, G.J. (1998) Comparison of Neon Like Germanium Inner Shell and Nickel Like Gadolinium at 62 A and 66 A by Picosecond Heating of a Performed Plasma. *Optics Communications*, **153**, 164-171.

[9] Norton, B.A. and Peacock, N.J. (1975) Population Inversion in Laser-Produced Plasmas by Pumping with Opacity-Broadened Lines. *Journal of Physics B*, **8**, 989. http://dx.doi.org/10.1088/0022-3700/8/6/026

[10] Bhagavatula, V.A. (1976) Soft X-Ray Population Inversion by Resonant Photoexcitation in Multicomponent Laser Plasmas. *Journal of Applied Physics*, **47**, 4535. http://dx.doi.org/10.1063/1.322425

[11] Nilsen, J., Beiersdorfer, P., Elliott, S.R., Phillips, T.W., Bryunetkin, B.A., Dyakin, V.M., Pikuz, T.A., Faenov, A.Ya., Pikuz, S.A., von Goeler, S., Bitter, M., Loboda, P.A., Lykov, V.A. and Politov, V.Yu. (1994) article title. *Physical Review A*, Article ID: 502143.

[12] Qi, N. and Krishnan, M. (1988) Enhancement of Ultraviolet Laser Plasma Emission Produced in a Strong Static Electric Field. *Optics Communications*, **67**, 124-128.

[13] Feldman, U., Bhatia, A.K. and Suckewer, S. (1983) Short Wavelength Laser Calculations for Electron Pumping in Neon-Like Krypton (Kr XXVII). *Journal of Applied Physics*, **54**, 2188. http://dx.doi.org/10.1063/1.332371

[14] Feldman, U., Seely, J.F. and Bhatia, A.K. (1984) Scaling of Collisionally Pumped 3s-3p Lasers in the Neon Isoelectronic Sequence. *Journal of Applied Physics*, **56**, 2475. http://dx.doi.org/10.1063/1.334308

[15] Chapline, G. and Wood, L. (1975) X-Ray Lasers. *Physics Today*, **28**, 40. http://dx.doi.org/10.1063/1.3069004

[16] Vinogradov, A.V. and Shlyaptsev, V.N. (1980) Calculations of Population Inversion Due to Transitions in Multiply Charged Neon-Like Ions in the 200-2000 Å Range. *Soviet Journal of Quantum Electronics*, **10**, 754. http://dx.doi.org/10.1070/QE1980v010n06ABEH010287

[17] Goldstein, W.H., Oreg, J., Zigler, A., Bar-Shalom, A. and Klapisch, M. (1988) Gain Predictions for Nickel-Like Gadolinium from a 181-Level Multiconfigurational Distorted-Wave Collisional-Radiative Model. *Physical Review A*, **38**, 1797. http://dx.doi.org/10.1103/PhysRevA.38.1797

[18] Sobel'man, I.I. (1979) Introduction to the Theory of Atomic Spectra, International Series of Monographs in Natural Philosophy. Vol. 40, Pergamon Press, Oxford.

[19] Hagelstein, P.L. (1986) Relativistic Distorted-Wave Results for Nickel-Like Gadolinium. *Physical Review A*, **34**, 874. http://dx.doi.org/10.1103/PhysRevA.34.874

[20] Zhang, H.L., Samson, D.H. and Fontes, C.J. (1991) Relativistic Distorted-Wave Collision Strengths and Oscillator

Strengths for the 33 Ni-Like Ions with 60 ≤ Z ≤ 92. *Atomic Data and Nuclear Data Tables*, **48**, 91-163. http://dx.doi.org/10.1016/0092-640X(91)90024-X

[21] Feldman, U., Doschek, G.A., Seely, J.F. and Bhatia, A.K. (1985) Short Wavelength Laser Calculations for Electron Pumping in Be I and B I Isoelectronic Sequences (18 ≤ Z≤ 36). *Journal of Applied Physics*, **58**, 2909. http://dx.doi.org/10.1063/1.335838

[22] Hibbert, A., Ledourneuf, M. and Mohan, M. (1993) Energies, Oscillators Strengths, and Life Times for Neon-Like Ions up to Kr XXVII. *Atomic Data and Nuclear Data Tables*, **53**, 23-112.

[23] Daido, H., Kodama, R., Murai, K., Yuan, G., Takagi, M., Kato, Y., Choi, I.W. and Nam, C.H. (1995) Significant Improvement in the Efficiency and Brightness of the J = 0-1 19.6-nm Line of the Germanium Laser by Use of Double-Pulse Pumping. *Optics Letters*, **20**, 61-63.

[24] NIST. http:///F:/NIST/NIST%20ASD%20Levels%20Output32.htm